Communications in Physics, Vol. 28, No. 4 (2018), pp. 311-321
DOI:10.15625/0868-3166/28/4/13099

EVALUATION OF SIMULTANEOUS FITTING METHOD FOR β-DECAY HALF-LIVES AND β-DELAYED MULTI NEUTRON EMISSION PROBABILITIES DEVELOPED FOR THE BRIKEN EXPERIMENT

VI HO PHONG[1,2,†], SHUNJI NISHIMURA[2], LE HONG KHIEM[3,4]

[1]*Faculty of Physics, VNU University of Science, 334 Nguyen Trai, Thanh Xuan, Hanoi*

[2]*RIKEN Nishina Center, 2-1 Hirosawa, Wako, Saitama 351-0198, Japan*

[3]*Institute of Physics, Vietnam Academy of Science and Technology, 10 Dao Tan, Ba Dinh, Hanoi, Vietnam*

[4]*Graduate University of Science and Technology, Vietnam Academy of Science and Technology, 18 Hoang Quoc Viet, Cau Giay, Hanoi, Vietnam*

[†]*E-mail:* phong@ribf.riken.jp

Received 16 September 2018
Accepted for publication 29 October 2018
Published 15 December 2018

Abstract. *This paper presents a Monte-Carlo code to simulate the time sequences of the β-decay following implantation of a continuous radioactive ion beam into a segmented silicon detector. We extended our simulation to the β-delayed neutron process. An analysis procedure, which has been developed to obtain simultaneously the β-decay half-life and the β-delayed multi-neutron emission probability, was verified by the simulation data.*

Keywords: Analysis methodology, Beta-delayed neutrons, Monte-Carlo simulation.

Classification numbers: 24.10.Lx;23.40.-s.

I. INTRODUCTION

The β decay of radioactive nuclei is one of the most fundamental weak-interaction process that occurs in the universe and across the chart of nuclei. An important property of the β decay is the characteristic half-life ($T_{1/2}$), which is often the first experimentally accessible quantity for radioactive nuclei far from stability. The measurement of the β-decay half-life of the radioactive isotopes (RI) has attracted considerable attention in the field of nuclear structure, nuclear astrophysics and fundamental electroweak standard model. In particular, β decay half-life measures the integration of so-called β strength function, which reflects the structure of the final state in daughter nuclei. The half-life of the proton-deficient nuclei is also an important physical parameter that modulates the speed of the r-process, the main mechanism for synthesis of heavy elements during the stellar evolution. Moreover, high precision measurement of β decay half-life of "superallowed" Fermi β decay type provides additional test of the CKM unitary within Electroweak Standard Model [1, 2]. Among these fields, the accurate measurement of the half-life of the very exotic nuclei is desired. However, such measurement often suffers the low counting rate and involves complicated components arising from descendant decay processes, which can be the main source of the uncertainty budget. Therefore, the simulation of the backgrounds and nuclear decay is needed to verify the analytical method and to obtain a reliable value of the half-life.

As for the β-decay half-life of the short-lived radioactive nuclei, with the recent development of the radioactive isotope beam facility, there exists two main techniques, of which typical measurable half-life ranges from micro-seconds to seconds. In the Isotope-Separation on-line (ISOL) facility with a tape transport system, the activation technique is employed where the accumulated and disintegrated β activities are counted by a single-pad silicon or a plastic scintillation detector [3, 4]. In the in-flight facility with fast-beam mass-separator, a high granularity silicon detector is often employed [5–7]. The main advantage of using such detector is that more than one isotope can be measured simultaneously by implanting a cocktail beam in to its active area. Recent advance in such measurement technique utilizes the double-sided silicon strip detector (DSSD) capable of recording both position and time information of the nuclei of interest and their β decay. By employing the neutron detector and digital electronics system, it is possible to perform single or double coincidence measurement of ion-β-neutron or ion-β-gamma, in which $T_{1/2}$ can be obtained with higher accuracy than that of a single ion-β measurement.

Beta-decay process is often followed by the emission of electromagnetic radiation or delayed particles due to the subsequent de-excitation of daughter nuclei. In neutron-rich nuclei, the delayed neutrons (DNs) emission process occurs when the β decay populates an excited state above the neutron separation energy. The β-delayed multi-neutron emission probabilities, P_{xn} (where $x = 1,\ 2,\ 3,\ \ldots$), characterizing the emission of x neutrons (βxn), are the characteristic quantities of this decay process. These values are of important for various fields. In nuclear physics, the P_{xn} value represents a fraction of β decay strength at the excitation energy above the neutron separation energy in daughter nuclei. In nuclear astrophysics, the DNs emission occurs along the decay of the r-process nuclei and it is an important process during the freeze-out time [8]. The DNs emission from fission product in nuclear reactor also plays a key role to control and operate the reactor safety [9].

Despite decades of extensive experimental efforts, the information about the DNs process has been mostly limited to the radioactive nuclei closed to stability and single-delayed neutron emission. Only about 298 P_{1n} values were measured out of 612 β-delayed neutron emitters listed in the Atomic Mass Evaluation (AME2016) [10, 11]. However, there exists a lot of discrepancies among the reported results which associated with large uncertainty due to experimental uncertainties in identification of associated neutrons with energies of a few eV up to a few MeV from the background in complex decay processes [4].

One limitation for the measurement of the P_{xn} values is the complex contributions from various sources of uncorrelated neutron-like background, namely: (i) electronics noise (ii) ambient background (mainly from cosmic days and natural radioactive nuclei) (iii) beam-induced neutrons (iv) beta-delayed neutron from others implanted isotopes from the cocktail beam.

Monte-Carlo simulation method has been successfully applied to study the radioactive decay processes. Examples include the simulation of the radioactive decay which was incorporated in the general-purpose Geant4 [12], MCNP [13] or FLUKA [14] programs. However, these programs are not suitable for simulating the complexity of the experimental setup in the radioactive beam facilities, including the effect of the background from electronics noises and the spatial distributions. Therefore, a Monte Carlo simulation program, which is specifically designed for the experimental setup in RIs beam facilities is needed to help verify the analysis procedure and understand the effect of background.

In this paper, Monte-Carlo technique was employed to obtain time-ordered implant-β and neutron data set simulating the experimental condition of a β-delayed neutron emission measurement in the fast-radioactive beam facility. A multicomponent fitting procedure to deduce simultaneously the β decay half-life and β-delayed multi-neutron emission probability was developed and verified by using the simulation data set.

II. EXPERIMENT

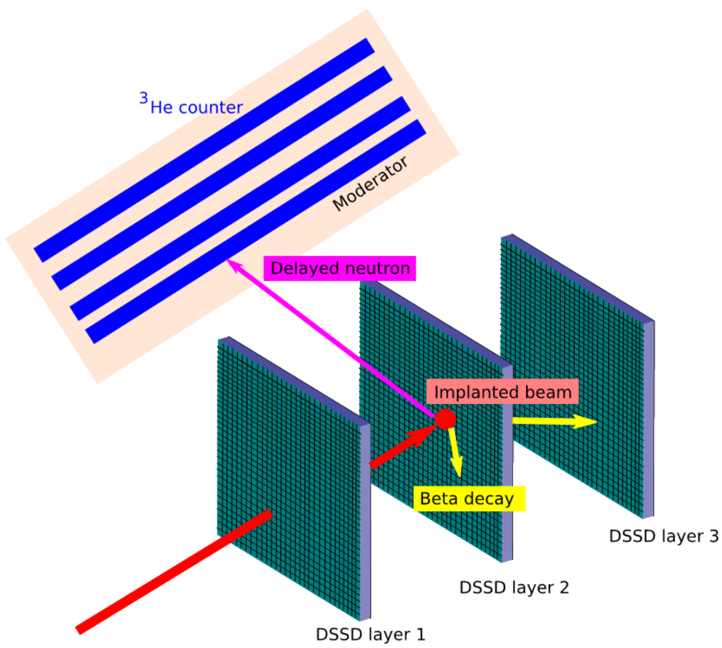

Fig. 1. Schematic view of the experimental setup for the measurement of β decay half-life and β delayed neutron emission probability.

The simulation described in the present work is motivated by an experimental program at RIKEN, the BRIKEN project [10], on the measurement of the $T_{1/2}$ and P_{xn} values of β-delayed neutron emitters in the neutron-rich region of the nuclear chart. The RIs beam was produced by fragmentation of the accelerated heavy ion beam impinged on a light target. Those isotopes were separated and identified event-by-event by using multi-stage spectrometer before entering the β decay setup described in Fig. 1. The setup consists of a stack of double-sided silicon detectors

(DSSDs) surrounded by a neutron counters array. The implantation of RIs beam and their subsequence β decay that took place in a segment of the DSSDs were recorded by a dual-gain electronic system and a time-stamping DAQ system. The detection of DNs following the β decay is realized by a neutron counters array, in which neutrons were slowed down in a high-density polyethylene block (moderator) until being captured in the ^{3}He counters. The design of this detector array can be found in [15]. The output raw data of the implant, beta and neutron events contains both the timing and spatial position, thanks to the digital electronics and time-stamping system.

III. SIMULATION PROCEDURE

The implantation events of the RIs in a DSSD detector were simulated with information about the time and spatial position. Their absolute arrival time was sampled randomly with an assumption of the Poisson process so that the time difference between successive events is described as a well-known exponential probability distribution

$$\Delta T_{implant} = e^{-Rt} \tag{1}$$

where R is the implantation rate.

The implantation position within an active detector area was simulated with a predefined distribution within a detector area to mimic the realistic implantation distribution due to the beam optics. Fig. 2a shows an example of the spatial distribution.

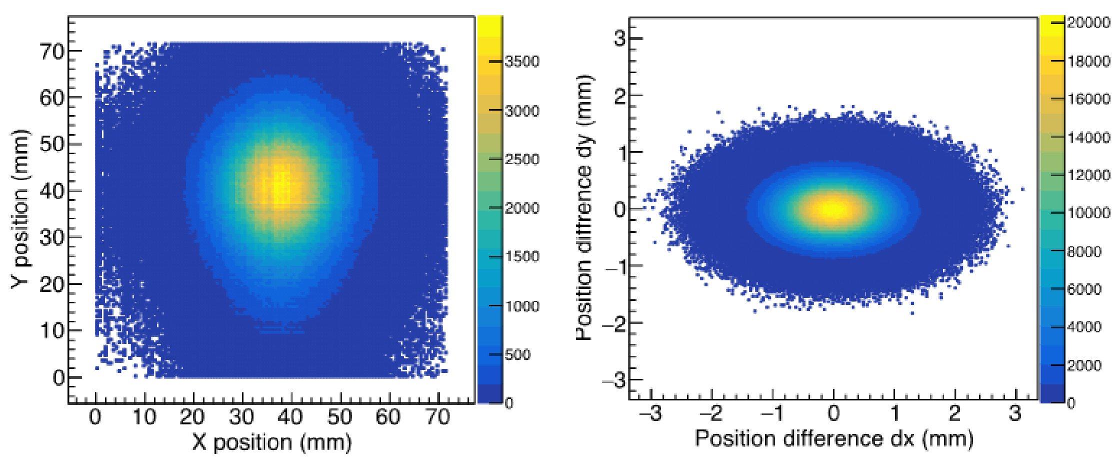

(a) (b)

Fig. 2. Simulated implantation profile (a) and the position difference dx and dy between detected decay event and implantation event (b).

After the implantation of each parent isotope in the DSSDs, β-decay event takes place after a time interval dT, which was randomly sampled from the exponential time distribution, where $T_{1/2}$ is the half-life of the parent nuclei:

$$dT = e^{-t(\ln 2)/T_{1/2}}. \tag{2}$$

These simulated time intervals were applied to all member in the decay chain, after their creation by β decay of the preceding (parent) nuclei. The decay chain including DNs emission branch, which were considered in the simulation, is demonstrated in Fig. 3. Simultaneously, the absolute timing information for each decay event was registered, sorted and stored in a form of specified data structure.

The emitted β particle from the decay events deposits its energy at the near-by position from the implantation position of RI. Their detection positions were sampled randomly assuming a predefined spatial distribution of the detected β particle around the implantation position in two dimensions (dx and dy) as shown in Fig. 2b. This is to mimics the ambiguity of the position determination of β particle due to the combined effect of strip threshold, the implantation depth and the small energy loss of β particle.

A certain portion of all beta events associated with the implanted RI is not detected by DSSSD due to the escape of the beta particles from the DSSSD, the electronics energy-threshold, and dead-time effect. The effects of in-efficiency were simulated by registering the events with a generated uniform-random number (from zero to unity) that falls within a given range of efficiency.

Upon the emission of the β particles from the decay chain members, the probability of emitting a neutron and its detection probability were simulated by a similar manner with the detection efficiency simulation for beta particles, given by the input values of β-delayed neutron emission probabilities and neutron detection efficiency for each decay chain member.

The β-like background arose from the implantation of the other isotopes and electronics noise were considered with an assumption of constant rate. Therefore, their absolute arrival times can be simulated in the same way with the primary implantation events. Moreover, their spatial distribution was also simulated with a predefined distribution.

In this work, the generation of the exponential, normal and uniform random number utilizes the TRandom3 class provided in the ROOT package [16].

IV. ANALYSIS PROCEDURE

The β-decay half-life was deduced by using the delayed coincidence method [6,18], where the time difference between an implantation of a particular isotope and the associated β-decay event was sorted into a time histogram of so-called decay curve, which describes the number of nuclei decaying in a unit time as a function of time. In order to reduce the random correlated background due to the decay of other implanted isotopes and electronics noise, a spatial correlation condition was applied by selecting the β-decay event at nearby position with respect to the implantation position. By fitting the resulting experimental decay curve to a mathematical formula, the β-decay half-life of the implanted nuclei was obtained.

Since the RIs of interest are far away from stability line in this work, the resulting decay curve was contributed by not only parent-daughter decay but also others decay products along the decay chain originated from parent nuclei as demonstrated in Fig. 3. The mathematical formula describing the decays of the nuclei in the decay chain superposed on a constant background C is given by:

$$f_b = \sum_{i=1}^{i=n} (\varepsilon_{\beta i} \lambda_i X_i(t)) + C \tag{3}$$

where $X_i = \sum_k X_k$ is the number of nuclei of ith member of the decay chain at certain time which is summed over all possible decay path k through β0n or βxn decay channels. λ_i and $\varepsilon_{\beta i}$ are the decay constant and the beta detection efficiency, respectively. In this work, we assumed a common β detection efficiency for all members in the decay chain as well as for the DNs emission channel as in [6, 19]. Thus, all contributions of the decaying nuclei are affected by the same efficiency factor and the resulting fit to the decay curve is independent of the β efficiency.

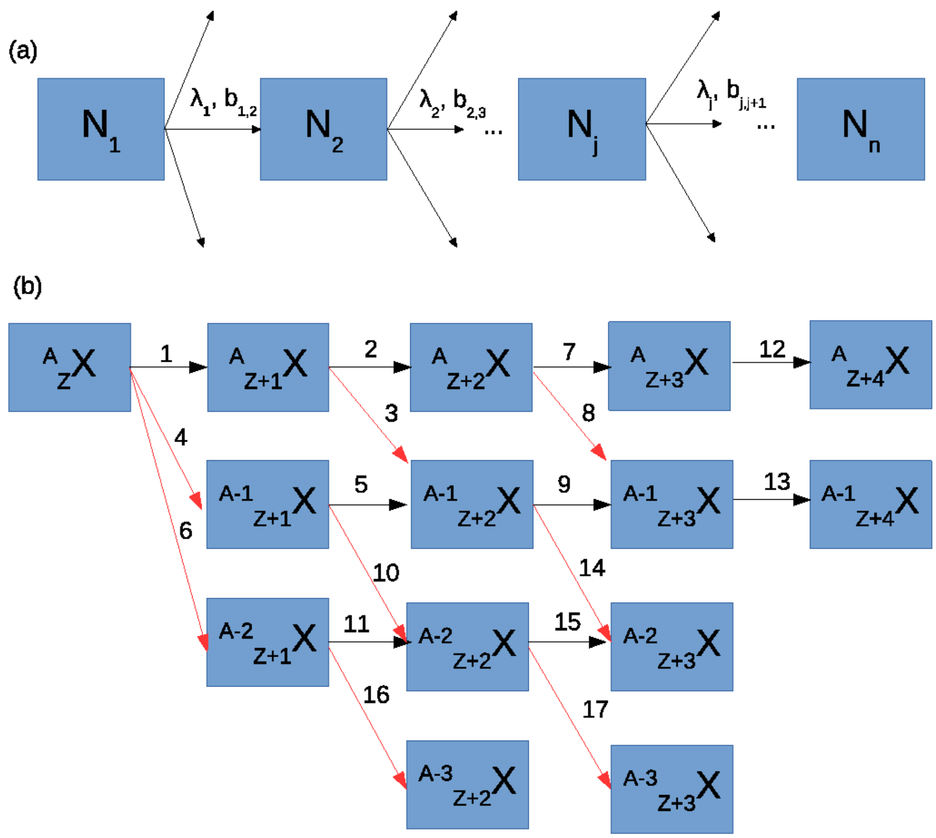

Fig. 3. A generalized flow path involving production and destruction of a member N_j in series with corresponding total removal constant λ_j and branching ratio b_j [17] (a) and an abstract flow diagram of a decay chain considered in the simulation, starting from an implantation of nuclei ${}^{A}_{Z}X$, the red arrows indicate the decay channel with delayed neutron emission (b).

The number of decaying nuclei for each linear decay path (as in Fig. 3) can be written explicitly by using a general solution of Batemann equations [17]:

$$X_i^k(t) = X_1(0)\left(\prod_{j=1}^{j=n-1} \lambda_j b_{j,j+1}\right)\sum_{j=1}^{j=n} \frac{e^{-\lambda_j t}}{\prod\limits_{p=1,p\neq j}^{p=n} \lambda_p - \lambda_j} \tag{4}$$

where $X_1(0)$ is the number of parent nuclei at time zero. λ_j and $b_{j,j+1}$ are the decay constant and the branching ratio of ith member in the decay chain.

The β-delayed neutron emission probabilities P_{xn} for a given implanted nucleus can be extracted by taking the ratio between the number of β-decay following by the delayed neutron emission and the total number of β decay. Those numbers were indirectly quantified by fitting the decay curves constructed from the implant-associated β-decay events in coincidence with neutron signal detected within a neutron thermalization time window T_{th} in the neutron counter, where appropriate fitting function was applied to follow the relation between the P_{xn} and the initial activities of parent nuclei with neutron multiplicity (gated for decay activities). For the $\beta 1n$ decay, the decay curve constructed in coincidence with single neutron event (multiplicity one) d_{1n} was used in the fit, whereas for β2n decay, we introduced an additional decay curve gated on two neutrons event (multiplicity two) d_{2n}. Within the context of this work, we concentrated only on the β-delayed one and two-neutron emitters which are of interest in the present experiment. Additional decay curves with gate on event with x neutrons emission $(x > 2)$ must be taken into account for determining P_{xn} with $x > 2$.

To begin with, let us assume an ideal case where there is no neutron background. The contribution to the one neutron gated decay curve d_{1n} comes from not only the $\beta 1n$ channel but also the $\beta 2n$ channel where only one out of two neutrons are detected in the neutron counter due to the detection inefficiency effect. The corresponding fitting function $f_{1n}(t)$ for d_{1n} (without a constant background) in this case is given by the following equations, where the first and the second summation run over all the β-delayed one and two neutron emitters in the decay chain, respectively

$$f^1_{\beta 1n}(t) = \sum_{i\in\beta 1n} P_{1n}\varepsilon_{\beta 1n}\varepsilon_{1n}\lambda_i X_i \tag{5}$$

$$f^2_{\beta 1n}(t) = \sum_{i\in\beta 2n} \varepsilon_{\beta 2n}2\varepsilon_{2n}(1-\varepsilon_{2n})P^i_{2ni}\lambda_i X_i(t) \tag{6}$$

$$f_{\beta 1n}(t) = f^1_{\beta 1n}(t) + f^2_{\beta 1n}(t) \tag{7}$$

The parameters ε_{1n} and ε_{2n} are the β efficiency for the delayed one and two neutrons channel, respectively. Within the context of this work, we assumed a common single neutron detection efficiency for β1n and β2n channels because of the constant detection efficiency of neutron with energies up to a few MeV for the BRIKEN project [10]. The systematic effect of possibly lower detection efficiency of neutron with higher energies ($E_n \geq 2$ MeV) will be described in a separate paper using the neutron hit distribution in the moderator.

The fitting function for two neutron gated decay curve d_{2n} (without a constant background) takes the form:

$$f_{\beta 2n}(t) = \sum_{i\in\beta 2n} P_{2n}\varepsilon^2_{2n}\lambda_i X_i(t) \tag{8}$$

Various background sources affect the experimental decay curves and must be taken into account in the fit. The accidental implant-β background comes from β-like signals detected in the DSSDs which are not associated with the implanted nuclei. This background contributes to the decay curves with and without neutron gate as a form of flat distribution superposed on the truly correlated implant-β signal. Such uncorrelated background component can be estimated by constructing the implant-β correlation in backward $(t < 0)$ time direction and extrapolate to the forward $(t > 0)$ direction by fitting it with a constant background model.

The random neutron background in coincidence with correlated implant-β events should be also considered in the fit of the d_{1n} and d_{2n} decay curves. The random coincidence probability factors are denoted by r_n for the probability of at least one random background neutron detected in coincidence, r_{1n} for the probability of one background neutron detected, and r_{2n} for the probability of two random background neutrons detected within T_{th}. The magnitude of these factors can be reliably obtained by taking the ratio between the number of neutron multiplicity (at least one, one or two neutrons) correlated β-like signals in backward ($t < 0$) time direction within the time window T_{th} and total number of β-like signals. For the singly neutron gated decay curve d_{1n}, the following three components should be considered:

1) The probability of that within the β -neutron correlation time window T_{th} there is exactly one background neutron detected (O_{1nbkg}) and no real neutrons from βxn decay are detected ($\overline{O_{real}}$):

$$\overline{O_{real}} \otimes O_{1nbkg} = r_{1n} f_\beta - r_{1n} f_{\beta 1n} - r_{1n} f_{\beta 2n} \tag{9}$$

2) The probability of that within the β -neutron correlation time window T_{th} there is exactly one real neutron from β1n decay detected (O_{1nreal}) and no background neutrons are detected ($\overline{O_{nbkg}}$):

$$O_{1nreal} \otimes \overline{O_{nbkg}} = f^1_{\beta 1n} - r_n f^1_{\beta 1n} \tag{10}$$

3) Similarly, for the case when there is exactly one real neutron from $\beta 2n$ decay detected ($O_{2n1real}$) and no background neutrons are detected ($\overline{O_{nbkg}}$) within the thermalization time T_{th}:

$$O_{2n1real} \otimes \overline{O_{nbkg}} = f^2_{\beta 1n} - r_n f^2_{\beta 1n} \tag{11}$$

The doubly neutron gated decay curve d_{2n} consists of four components as described below:

1) The probability of that within the β-neutron correlation time window T_{th} there is exactly two background neutrons (O_{2nbkg}) detected and no real neutrons from βxn (O_{real}) are detected

$$\overline{O_{real}} \otimes O_{2nbkg} = r_{2n} f_\beta - r_{2n} f_{\beta 1n} - r_{2n} f_{\beta 2n} \tag{12}$$

2) The probability of that within the β-neutron correlation time window T_{th} there is exactly two real neutrons from β2n decay detected (O_{2nreal}) and no background neutrons are detected ($\overline{O_{nbkg}}$):

$$O_{2nreal} \otimes \overline{O_{nbkg}} = f_{\beta 2n} - r_n f_{\beta 2n} \tag{13}$$

3) The probability of that within the β-neutron correlation time window T_{th} there is exactly one real neutron from β1n decay detected (O_{1nreal}), together with one background neutron (O_{1nbkg}) and no others background neutron are detected ($\overline{O_{nbkg}}$):

$$(O_{1nreal} \otimes O_{1nbkg}) \otimes \overline{O_{nbkg}} = r_{1n} f^1_{1n} - r_n (r_{1n} f^1_{1n}) \tag{14}$$

4) Similarly, for the case when exactly one real neutron from β2n decay detected ($O_{2n1real}$), together with one background neutron (O_{1nbkg})and no other background neutron are detected ($\overline{O_{nbkg}}$):

$$(O_{2n1real} \otimes O_{1nbkg}) \otimes \overline{O_{nbkg}} = r_{1n} f^2_{1n} - r_n (r_{1n} f^2_{1n}) \tag{15}$$

V. RESULTS AND DISCUSSION

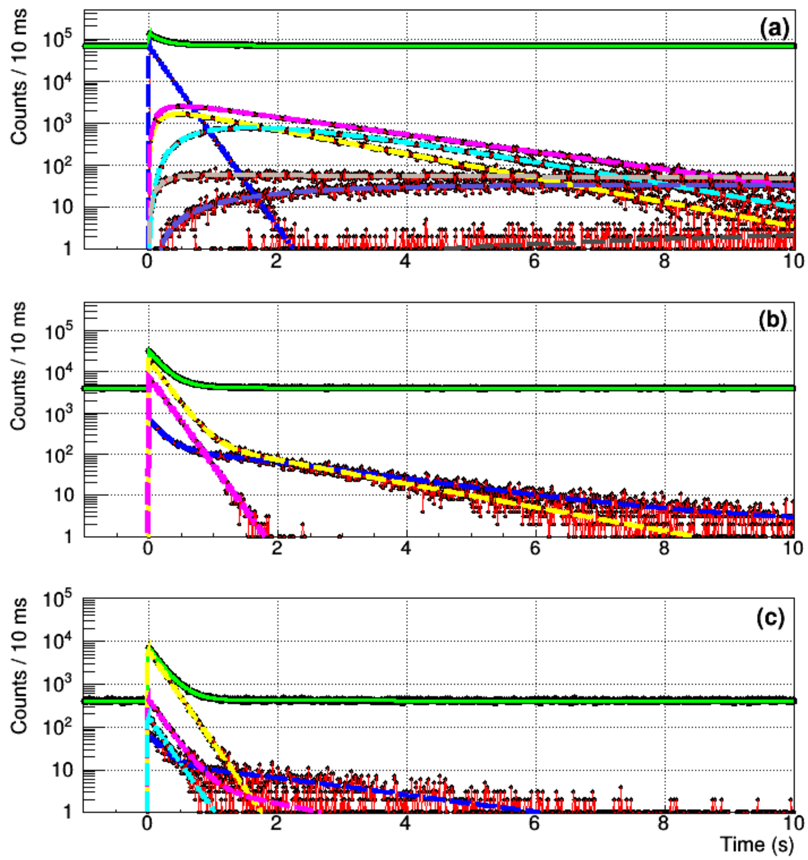

Fig. 4. (Color online) Results of the simultaneous analysis of $T_{1/2}$, P_{1n} and P_{2n} of ^{134}In. In presented in the form of decay curves without neutron gate (a), with one neutron gate (b) and two neutrons gate (c). In panel (a) the green solid line represents the combined fitting function, other dashed- lines represent decay components of parent (blue dashed line) and descendant nuclei in the decay chain. In panel (b), the green solid line represents the combined fitting functions of component 1 (yellow dashed line), component 2 (blue dashed line), component 3 (purple dashed line) and background. In panel (c) the green solid line represents the combined fitting function of component 1 (yellow dashed line), component 2 (purple dashed line), component 3 (cyan dashed line), component 4 (blue dashed line) and background. The decomposition of each components from simulation data as a form of histogram were displayed as well. Details explanation of each components were presented in Sec. IV.

The consistency check of results can be assessed by applying the analysis method to the simulation data sets that have been generated from known input parameters. In this paper, the simulated data set were made for the analysis of the β-delayed neutron measurement of the very neutron rich nuclei around $N = 82$ neutron shell closures. Here, we took an example of the expected β-delayed two neutrons emitter ^{134}In [20]. The $T_{1/2}$ and P_{xn} values of descendant nuclei and the $T_{1/2}$ of parent nuclei (140(4) ms) used in the simulation were taken from NNDC database [21]. To mimic an extreme condition of the neutron and β background, the experimental condition such as the implantation rate, neutron and β background rate for the nuclei with largest implantation rate was taken as input parameters for the simulation. We generated a simulation data set assuming two hypothetical scenarios for P_{xn} values of parent nuclei: (1) $P_{1n} = 50\%$ and $P_{2n} = 50\%$, (2) P_{1n} = 50% and P_{2n} = 25%. The simulated data set were sorted into three decay curves: without gating on neutron d, gating on neutron multiplicity one d_{1n} and gating on neutron multiplicity two d_{2n}. They were then fitted simultaneously by Binned Maximum-Likelihood method, which is incorporated in the ROOT package. The $T_{1/2}$, P_{1n}, P_{2n}, the initial activity and constant background are only parameters that were varied in the fit.

Figure 4a shows the fitted decay curves. In this figure, each decay components of descendant nuclei can be decomposed thank to the capability to identify temporal position in the decay chain of each neutron and beta events from the simulated data set. In Fig. 4b and Fig. 4c, the fitted decay curves gated with one and two neutrons were presented together with their decomposition of each contributed components as mentioned earlier. The best estimate of the $T_{1/2}$ and P_{1n} and P_{2n} values for the first case were 140.2(3) ms, 50.1(2)% and 50.05(16) %, respectively. While for the second case we obtained $T_{1/2} = 140.1(3)$, $P_{1n} = 49.9(2)\%$ and $P_{2n} = 25.07(12)\%$. The perfect agreement of the analytical fitting functions with the decay curves with and without neutron multiplicity gating demonstrates the capability of the analysis method to provide best estimates for the $T_{1/2}$ and P_{xn} values, which are also confirmed to be matched with the simulation input parameters within the statistical error.

VI. CONCLUSION

In this work, we have introduced a new simulation algorithm to simulate a typical β-decay measurement in the fast-radioactive beam facility utilizing highly segment implantation detector and neutron counter array. A sophisticated analysis method was developed to extract simultaneously the $T_{1/2}$, P_{1n} and P_{2n} values from the time-stamped data set. The simulation data set of ^{134}In under extreme condition of neutron and β background were used to confirm the validity of our analysis procedure.

The success of our analysis method will be also applicable for high precision decay spectroscopy with additional coincidence of gamma-rays in future.

ACKNOWLEDGMENT

The authors acknowledge fruitful discussions with BRIKEN collaborators during the experiment and the data analysis process. V.P would like to express great gratitude to the RIKEN institute for the support during the term of IPA program at RIKEN Nishina Center. This work was supported by JSPS KAKENHI (Grants Numbers 14F04808, 17H06090, 25247045, 19340074). One of the authors L. H. Khiem also acknowledges the Vietnam Academy of Science and Technology for the support under the projects named “Development of computing science for specialized fields based on Resource Sharing High Performance Computing Center at VAST” and “Study of unstable nuclei beam induced nuclear reactions at RIKEN” under the Program of Development in the field of Physics by 2020.

REFERENCES

[1] A. Morales, A. Algora, B. Rubio, K. Kaneko, S. Nishimura, P. Aguilera, S. Orrigo, F. Molina, G. DeAngelis, F. Recchia *et al.*, *Physical Review C* **95** (2017) 064327.

[2] J.C.Hardyand, I.S.Towner, *Annalen der Physik* **525** (2013) 443.

[3] J.Agramunt, J.Tain, M.B.Gomez-Hornillos, A.Garcia, F.Albiol, A.Algora, R.Caballero-Folch, F.Calvino, D.Cano-Ott, G.Cortes et al., *Nuclear Instruments and Methods in Physics Research Section A: Accelerators, Spectrometers, Detectors and Associated Equipment* **807** (2016) 69.

[4] L.Mathieu, O.Serot, T.Materna, A.Bail, U.Koster, H.Faust, O.Litaize, E.Dupont, C.Jouanne, A.Letourneau et al., *Journal of Instrumentation* **7** (2012) P08029.

[5] J. Prisciandaro, A. Mortonand, P. Mantica, *Nuclear Instruments and Methods in Physics Research Section A: Accelerators, Spectrometers, Detectors and Associated Equipment* **505** (2003) 140.

[6] C. Hinke, M. Bohmer, P. Boutachkov, T. Faestermann, H.Geissel, J. Gerl, R. Gernhauser, M. Gorska, A. Gottardo, H. Grawe *et al.*, *Nature* **486** (2012) 341.

[7] S. Nishimura, G.Lorusso, Z.Xu et al., *Prog. Rep* **46** (2013) 182.

[8] R. Surman, M.Mumpower, and A.Aprahamian, *The sensitivity of γ-process nucleo synthesis to individual β-delayed neutron emission probabilities*, Proceedings of the Conference on Advances in Radioactive Isotope Science (ARIS2014), 2015, p.010010.

[9] A. Michaudon, *Computation and Analysis of Nuclear Data Relevant to Nuclear Energy And Safety* (1993) 244.

[10] I. Dillmannand, A. Tarife no-Saldivia, *Nuclear Physics News* **28**(2018) 28.

[11] M. Wang, G. Audi, F. Kondev, W. Huang, S. Naimi and X. Xu, *Chinese Physics C* **41** (2017) 030003.

[12] S. Agostinelli, J. Allison, K. A. Amako, J. Apostolakis, H. Araujo, P. Arce, M. Asai, D. Axen, S. Banerjee, G. Barrand *et al.*, *Nuclear instruments and methods in physics research section A: Accelerators, Spectrometers, Detectors and Associated Equipment* **506** (2003) 250–303.

[13] J. F. Briesmeister, *LA-12625* (1993).

[14] A. Ferrari, P. R. Sala, A. Fasso and J. Ranft, *Fluka: A multi-particle transport code (programversion 2005)*, Tech. Report, 2005.

[15] A. Tarifeno-Saldivia, J.Tain, C.Domingo-Pardo, F.Calvino, G.Cortes, V. Phong, A. Riego, J. Agramunt, A. Algora, N. Brewer *et al.*, *Journal of Instrumentation* **12** (2017) P04006.

[16] R. Brun, and F. Rademakers, *Nuclear Instruments and Methods in Physics Research Section A: Accelerators, Spectrometers, Detectors and Associated Equipment* **389** (1997) 81–86.

[17] K. Skrable, C. French, G. Chabot and A. Major, *Health physics* **27** (1974) 155–157.

[18] S.Pomme, *Metrologia* **52** (2015) S51.

[19] R.Caballero-Folch, C.Domingo-Pardo, J.Agramunt, A.Algora, F.Ameil, Y.Ayyad, J.Benlliure, M.Bowry, F.Calvino, D.Cano-Ott et al., *Physical Review C* **95** (2017) 064322.

[20] P. Moller, B. Pfeiffer, and K.-L.Kratz, *Physical Review C* **67** (2003) 055802.

[21] N. ENSDF, *online data service, endsf database*, 2015.